

Predictive Filtering for Attitude Estimation Without Rate Sensors

John L. Crassidis¹

F. Landis Markley²

Abstract

In this paper, a real-time predictive filter is derived for spacecraft attitude estimation without the utilization of angular rate measurements from gyros. The formulation described in this paper is shown using only attitude sensors (e.g., three-axis magnetometers, sun sensors, star trackers, etc.). The new real-time nonlinear filter predicts the required torque modeling error input in order to propagate the spacecraft dynamic model, so that model responses match the measured vector observations. Algorithms are developed which require the output estimates to track either the body measurements from the on-board sensors or the inertial reference trajectories generated from ephemeris data sets. The real-time predictive filter is used to estimate the attitude of the Solar, Anomalous, Magnetospheric Particle Explorer (SAMPEX) spacecraft. Results using this new algorithm indicate that the real-time predictive filter accurately estimates the attitude of an actual spacecraft with the sole use of magnetometer sensor measurements.

¹ NRC Resident Research Fellow, *Goddard Space Flight Center, Code 712, Greenbelt, MD 20771*. Member AIAA.

² Staff Engineer, *Goddard Space Flight Center, Code 712, Greenbelt, MD 20771*. Associate Fellow AIAA

Introduction

The attitude of a spacecraft can be determined by either deterministic methods or by utilizing algorithms which combine dynamic and/or kinematic models with sensor data. Three-axis deterministic methods, such as TRIAD (algebraic method) [1], QUEST [2], and FOAM [3], require measurements of at least two vectors to determine the attitude (direction-cosine) matrix. An advantage of both the QUEST and FOAM algorithms is that the attitude of a spacecraft can be estimated using measurements of more than two vectors. This is accomplished by minimizing a quadratic loss function first posed by Wahba [4]. However, all deterministic methods fail when only one set of vector measurements is available, (e.g., magnetometer data only). Estimation algorithms utilize dynamic and/or kinematic models and subsequently can (in theory) estimate the attitude of a spacecraft using a time series of measurements of a single vector. Although all spacecraft in use today have at least two on-board attitude sensors, estimation techniques can be used to determine the attitude during anomalous periods, such as solar eclipse and/or vector-measurement co-alignment.

The Kalman filter has been proven to be extremely useful for attitude estimation using vector attitude measurements and gyro measurements. The essential feature of the Kalman filter is the utilization of state-space formulations in the system model design. Errors in the dynamic model are treated as “process noise,” since system models are not usually improved or updated during the estimation process. The process noise is essentially used to shift the emphasis from the system model to the measurements. The Kalman filter satisfies an optimality criterion which minimizes the trace of the covariance of the estimate error between the system model responses and the actual measurements. Statistical properties of the process noise and measurement error sequence are used to determine an optimal filter design. Therefore, the model characteristics are combined with sequential measurements in order to obtain state estimates which meliorate both the measurements and model responses.

In the Kalman filter, the model error (process noise) is assumed to be modeled by a zero-mean Gaussian process with known covariance (e.g., ramp noise for gyro drift models). However, in actual practice the determination of the process noise covariance is usually obtained by an ad hoc and/or heuristic approach resulting in suboptimal filter designs. Also, in many

cases such as those with nonlinearities in the actual system (e.g., nonlinear torque models used in Euler's equation), the assumption of a Gaussian model error process can lead to severely degraded state estimates.

For spacecraft attitude estimation, the Kalman filter is most applicable to spacecraft equipped with three-axis gyros as well as attitude sensors [5]. However, gyros are generally expensive and are often prone to degradation or failure. Therefore, in recent years gyros have often been omitted (e.g., in Small Explorer (SMEX) spacecraft, such as SAMPEX). To circumvent the problem of gyro omission or failure, analytical models of rate motion can be used. This approach has been successfully used in a Real-Time Sequential Filter (RTSF) algorithm which propagates state estimates and error covariances using a dynamic model (see [6,7]). The estimation of dynamic rates by the RTSF is accomplished from angular momentum model propagation, and then correcting for these rates by using a "gyro bias" component in the filter design. A clear advantage of using dynamic models is shown for the case of near co-alignment of the spacecraft-to-sun and magnetic field vectors. For this case, deterministic algorithms, such as TRIAD and QUEST, show anomalous behaviors with extreme deviations in determined attitudes. Since the RTSF propagates an analytical model of motion, attitude estimates are improved even when data from only one attitude sensor is available. However, the RTSF is essentially a Kalman filter in which the "gyro bias" (and subsequently the angular momentum correction) is modeled as a Gaussian process with known covariance. Also, fairly accurate models of angular momentum are required in order to obtain accurate estimates. Subsequently, the design process for choosing the model error covariance becomes difficult. Other approaches to using a Kalman filter with no gyro data are discussed in reference [8].

Although the quaternion representation is the most commonly used for attitude estimation, the problem of maintaining proper normalization exists. This constraint leads to a singularity in the covariance matrix, which in actual practice is difficult to maintain due to linearization and/or computer round-off error. Three solutions (two of which yield identical results) to this problem are summarized by Lefferts et al. [5]. This paper also contains an extensive bibliography of earlier work on quaternion attitude estimation. Bar-Itzhack and Deutschmann show two further approaches to quaternion normalization (see [9] for details).

A new approach for performing optimal state estimation in the presence of significant model error has been developed by Mook and Junkins [10]. This algorithm, called the Minimum Model Error (MME) estimator, unlike most filter and smoother algorithms, does not assume that the model error is represented by a Gaussian process. Instead, the model error is determined during the MME estimation process. The algorithm determines the corrections added to the assumed model such that the model and corrections yield an accurate representation of the system behavior. This is accomplished by solving system optimality conditions and an output error covariance constraint. Therefore, accurate state estimates can be determined without the use of precise system representations in the assumed model. This algorithm has been successfully used to estimate the attitude of an actual spacecraft without the utilization of gyro measurements (see [8]). However, the MME estimator is a batch (off-line) estimator which must utilize post-experiment measurements.

The algorithm developed in this paper can be used to estimate the attitude of a spacecraft in real-time (as does the Kalman filter). However, the algorithm is not limited to the Gaussian noise characteristics for the model error. Essentially, this new algorithm combines the good qualities of both the Kalman filter (i.e., a real-time estimator) and the MME estimator (i.e., determines actual model error trajectories). The new algorithm is based on a predictive tracking scheme introduced by Lu [11]. Although the problem shown in [11] is solved from a control standpoint, the algorithm developed in this paper is reformulated as a filter and estimator with a stochastic measurement process. Therefore, the new algorithm is known as a predictive filter. The advantages of the new algorithm include: (i) the model error is assumed unknown and is estimated as part of the solution, (ii) the model error may take any form (even nonlinear), and (iii) the algorithm can be implemented on-line to both filter noisy measurements and estimate attitude and rate trajectories.

The organization of this paper proceeds as follows. First, a summary of the spacecraft attitude kinematics and sensor models is shown. Then, a brief review of the predictive filter for nonlinear systems is shown. Next, a predictive filter is developed for the purpose of attitude estimation. This approach determines the optimal spacecraft attitude in real-time by minimizing a quadratic cost function consisting of a measurement residual term and a model error term. A number of formulations is presented which estimate either for angular velocity or angular

momentum. Also, algorithms are developed which require the output estimates to track either the body measurements or the inertial reference trajectories. The inertial reference case avoids the need to take derivatives of noisy measurements. Finally, the predictive filter is used to estimate the attitude of SAMPEX in order to demonstrate the usefulness of this algorithm.

Attitude Kinematics and Dynamics

In this section, a brief review of the kinematic and dynamic equations of motion for a three-axis stabilized spacecraft is shown. The attitude is assumed to be represented by the quaternion, defined as

$$\underline{q} \equiv \begin{bmatrix} \underline{q}_{13} \\ q_4 \end{bmatrix} \quad (1)$$

with

$$\underline{q}_{13} \equiv \begin{bmatrix} q_1 \\ q_2 \\ q_3 \end{bmatrix} = \hat{n} \sin(\theta/2) \quad (2a)$$

$$q_4 = \cos(\theta/2) \quad (2b)$$

where \hat{n} is a unit vector corresponding to the axis of rotation and θ is the angle of rotation. The quaternion kinematic equations of motion are derived by using the spacecraft's angular velocity ($\underline{\omega}$), given by

$$\dot{\underline{q}} = \frac{1}{2} \Omega(\underline{\omega}) \underline{q} = \frac{1}{2} \Xi(\underline{q}) \underline{\omega} \quad (3)$$

where $\Omega(\underline{\omega})$ and $\Xi(\underline{q})$ are defined as

$$\Omega(\underline{\omega}) \equiv \begin{bmatrix} -[\underline{\omega} \times] & \vdots & \underline{\omega} \\ \dots\dots & \vdots & \dots\dots \\ -\underline{\omega}^T & \vdots & 0 \end{bmatrix} \quad (4a)$$

$$\Xi(\underline{q}) \equiv \begin{bmatrix} q_4 I_{3 \times 3} + [\underline{q}_{13} \times] \\ \dots\dots\dots \\ -\underline{q}_{13}^T \end{bmatrix} \quad (4b)$$

where $I_{3 \times 3}$ is a 3×3 identity matrix. The 3×3 dimensional matrices $[\underline{\omega} \times]$ and $[\underline{q}_{13} \times]$ are referred to as cross product matrices since $\underline{a} \times \underline{b} = [\underline{a} \times] \underline{b}$, with

$$[\underline{a} \times] \equiv \begin{bmatrix} 0 & -a_3 & a_2 \\ a_3 & 0 & -a_1 \\ -a_2 & a_1 & 0 \end{bmatrix} \quad (5)$$

Since a three degree-of-freedom attitude system is represented by a four-dimensional vector, the quaternions cannot be independent. This condition leads to the following normalization constraint

$$\underline{q}^T \underline{q} = \underline{q}_{13}^T \underline{q}_{13} + q_4^2 = 1 \quad (6)$$

Also, the matrix $\Xi(\underline{q})$ obeys the following helpful relations

$$\Xi^T(\underline{q}) \Xi(\underline{q}) = \underline{q}^T \underline{q} I_{3 \times 3} \quad (7a)$$

$$\Xi(\underline{q}) \Xi^T(\underline{q}) = \underline{q}^T \underline{q} I_{4 \times 4} - \underline{q} \underline{q}^T \quad (7b)$$

$$\Xi^T(\underline{q}) \underline{q} = \underline{0}_{3 \times 1} \quad (7c)$$

$$\Xi^T(\underline{q}) \underline{\lambda} = -\Xi^T(\underline{\lambda}) \underline{q} \text{ for any } \underline{\lambda}_{4 \times 1} \quad (7d)$$

where $\underline{0}_{3 \times 1}$ is a 3×1 zero vector. The dynamic equations of motion, also known as Euler's equations, for a rotating spacecraft are given by ([12])

$$\dot{\underline{H}} = \underline{N} - \underline{\omega} \times \underline{H} = \underline{J} \dot{\underline{\omega}} \quad (8)$$

where \underline{H} is the total angular momentum, \underline{N} is the total external torque (which includes, e.g., control torques, aerodynamic drag torques, solar pressure torques, etc.), and \underline{J} is the inertia matrix of the spacecraft. If reaction or momentum wheels are used on the spacecraft, the total angular momentum is given by

$$\underline{H} = J \underline{\omega} + \underline{h} \quad (9)$$

where \underline{h} is the total angular momentum due to the wheels. Thus, Equation (8) can be re-written as

$$\dot{\underline{H}} = \underline{N} - \left[J^{-1}(\underline{H} - \underline{h}) \right] \times \underline{H} \quad (10)$$

Also, from Equations (8) and (9) the following angular velocity form of Euler's equation can be used

$$J \dot{\underline{\omega}} = \underline{N} - \dot{\underline{h}} - \underline{\omega} \times (J \underline{\omega} + \underline{h}) \quad (11)$$

which involves the derivative of the wheel angular momentum.

The measurement model is assumed to be of the form given by

$$\underline{B}_B = A(\underline{q}) \underline{B}_I \quad (12)$$

where \underline{B}_I is a 3×1 dimensional vector of some reference object (e.g., a vector to the sun or to a star, or the Earth's magnetic field vector) in a reference coordinate system, \underline{B}_B is a 3×1 dimensional vector defining the components of the corresponding reference vector measured in the spacecraft body frame, and $A(\underline{q})$ is given by

$$A(\underline{q}) = (q_4^2 - \underline{q}_{13}^T \underline{q}_{13}) I_{3 \times 3} + 2 \underline{q}_{13} \underline{q}_{13}^T - 2 q_4 \left[\underline{q}_{13} \times \right] \quad (13)$$

which is the 3×3 dimensional (orthogonal) attitude matrix. A simpler form for the attitude matrix in Equation (13) is given by

$$A(\underline{q}) = -\Xi^T(\underline{q}) \Psi(\underline{q}) \quad (14)$$

where

$$\Psi(\underline{q}) \equiv \begin{bmatrix} -q_4 I_{3 \times 3} + \left[\underline{q}_{13} \times \right] \\ \dots\dots\dots \\ \underline{q}_{13}^T \end{bmatrix} \quad (15)$$

Also, another useful identity is given by

$$\Psi(q)\underline{\omega} = \Gamma(\underline{\omega})\underline{q} \quad \text{for any } \underline{\omega}_{3 \times 1} \quad (16)$$

where

$$\Gamma(\underline{\omega}) \equiv \begin{bmatrix} -[\underline{\omega} \times] & \vdots & -\underline{\omega} \\ \cdots & \vdots & \cdots \\ \underline{\omega}^T & \vdots & 0 \end{bmatrix} \quad (17)$$

Nonlinear Predictive Tracking

In this section, a brief review of the nonlinear predictive tracking algorithm first introduced by Lu [11] is shown. Although the problem shown in [11] is solved from a control standpoint, the algorithm developed in this section is reformulated as an estimator/filter with a stochastic measurement process. This development is based upon the duality which exists between control problems and estimation problems. In the nonlinear predictive filter it is assumed that the state and output estimates are given by a preliminary model and a to-be-determined model error vector, given by

$$\underline{\hat{x}}(t) = \underline{f}(\underline{\hat{x}}(t), t) + G(t)\underline{d}(t) \quad (18a)$$

$$\underline{\hat{y}}(t) = \underline{c}(\underline{\hat{x}}(t), t) \quad (18b)$$

where \underline{f} is a $n \times 1$ model vector, $\underline{\hat{x}}(t)$ is a $n \times 1$ state estimate vector, $\underline{d}(t)$ is a $l \times 1$ model error vector, $G(t)$ is a $n \times l$ model-error distribution matrix, \underline{c} is a $m \times 1$ measurement vector, and $\underline{\hat{y}}(t)$ is a $m \times 1$ estimated output vector. State-observable discrete measurements are assumed for Equation (18b) in the following form

$$\underline{\tilde{y}}(t_k) = \underline{c}(\underline{x}(t_k), t_k) + \underline{v}(t_k) \quad (19)$$

where $\underline{\tilde{y}}(t_k)$ is a $m \times 1$ measurement vector at time t_k , $\underline{x}(t_k)$ is the true state vector, and $\underline{v}(t_k)$ is a $m \times 1$ measurement noise vector which is assumed to be a zero-mean, Gaussian white-noise distributed process with

$$E\{\underline{v}(t_k)\} = \underline{0} \quad (20a)$$

$$E\left\{\underline{v}(t_k)\underline{v}^T(t_{k'})\right\} = R\delta_{kk'} \quad (20b)$$

where R is a $m \times m$ positive-definite covariance matrix.

A cost functional consisting of the weighted sum square of the measurement-minus-estimate residuals plus the weighted sum square of the model correction term is minimized, given by

$$J(t) = \frac{1}{2} \left\{ \underline{\tilde{y}}(t + \Delta t) - \underline{\hat{y}}(t + \Delta t) \right\}^T R^{-1} \left\{ \underline{\tilde{y}}(t + \Delta t) - \underline{\hat{y}}(t + \Delta t) \right\} + \frac{1}{2} \underline{d}^T(t) W \underline{d}(t) \quad (21)$$

where Δt is the measurement sampling interval, and W is a $l \times l$ weighting matrix. The necessary conditions for the minimization of Equation (21) lead to the following model error solution

$$\underline{d}(t) = - \left[\Lambda(\Delta t) S(\hat{x}) \right]^T R^{-1} \Lambda(\Delta t) S(\hat{x}) + W \Big]^{-1} \left[\Lambda(\Delta t) S(\hat{x}) \right]^T R^{-1} \left[\underline{z}(\hat{x}, \Delta t) - \underline{e}(t) - \underline{b}(t, \Delta t) \right] \quad (22)$$

where $\underline{e}(t) = \underline{\tilde{y}}(t) - \underline{\hat{y}}(t)$, $S(\hat{x})$ is a $m \times l$ dimensional matrix, and $\Lambda(\Delta t)$ is a $m \times m$ diagonal matrix with elements given by

$$\lambda_{ii} = \frac{\Delta t^{p_i}}{p_i!}, \quad i = 1, 2, \dots, m \quad (23)$$

where p_i is the lowest order of the derivative of $\hat{y}_i(t)$ in which any component of $\underline{d}(t)$ first appears in $\hat{x}(t)$. The i^{th} component of $\underline{z}(\hat{x}, \Delta t)$ is given by

$$z_i(\hat{x}, \Delta t) = \Delta t L_f^1(c_i) + \frac{\Delta t^2}{2!} L_f^2(c_i) + \dots + \frac{\Delta t^{p_i}}{p_i!} L_f^{p_i}(c_i), \quad i = 1, 2, \dots, m \quad (24)$$

where $L_f^k(c_i)$ is the k^{th} Lie derivative, defined by

$$\begin{aligned} L_f^k(c_i) &= c_i & \text{for } k = 1 \\ L_f^k(c_i) &= \frac{\partial L_f^{k-1}(c_i)}{\partial \hat{x}} \underline{f} & \text{for } k > 1 \end{aligned} \quad (25)$$

The i^{th} component of $\underline{b}(t, \Delta t)$ is given by

$$b_i(t, \Delta t) = \Delta t \tilde{y}_i(t) + \frac{\Delta t^2}{2!} \ddot{y}_i(t) + \dots + \frac{\Delta t^{p_i}}{p_i!} \tilde{y}_i^{(p_i)}(t), \quad i = 1, 2, \dots, m \quad (26)$$

The i^{th} row of $S(\hat{x})$ is given by

$$s_i = \left\{ L_{g_1} \left[L_f^{p_i-1}(c_i) \right], \dots, L_{g_l} \left[L_f^{p_i-1}(c_i) \right] \right\}, \quad i = 1, 2, \dots, m \quad (27)$$

where g_j is the j^{th} column of $G(t)$, and the Lie derivative is defined by

$$L_{g_j} \left[L_f^{p_i-1}(c_i) \right] \equiv \frac{\partial L_f^{p_i-1}(c_i)}{\partial \hat{x}} g_j, \quad j = 1, 2, \dots, l \quad (28)$$

Therefore, Equation (22) is used in Equation (18a) to propagate the state estimates to time t_k , then the measurement is processed at time t_k to find the new $\underline{d}(t)$ in $[t_k, t_{k+1}]$, and then the state estimates are propagated to time t_{k+1} .

The weighting matrix (W) in Equation (21) can be determined on the basis that the measurement-minus-estimate error covariance matrix must match the measurement-minus-truth error covariance matrix (see [10]). This condition is referred to as the ‘‘covariance constraint,’’ shown as

$$\frac{1}{m_{\text{tot}}} \sum_{k=1}^{m_{\text{tot}}} \left\{ \underline{\tilde{y}}(t_k) - \underline{\hat{y}}(t_k) \right\} \left\{ \underline{\tilde{y}}(t_k) - \underline{\hat{y}}(t_k) \right\}^T \approx R \quad (29)$$

where m_{tot} is the total number of measurement points. The covariance constraint is satisfied when the proper balance between model error and measurement residual has been achieved. If the measurement residual covariance is higher than the known measurement error covariance (R), then W should be decreased to less penalize the model error. Conversely, if the residual covariance is lower than the known covariance, then W should be increased so that less unmodeled dynamics are added to the assumed system model. The optimal weighting matrix is therefore obtained when the covariance constraint in Equation (29) is satisfied.

Attitude Estimation-Angular Momentum Case

In this section, a nonlinear predictive filter is derived for spacecraft attitude using the quaternion kinematic equations and the angular momentum version of Euler's equation. Two cases are presented. The first case utilizes the spacecraft body measurements as the desired tracking trajectories. The second case utilizes the inertial reference as the tracking trajectories. This case avoids the need to take derivatives of noisy measurements.

Body Measurement Case

The nonlinear predictive filter for this case minimizes the following cost function

$$J = \frac{1}{2} \left\{ \tilde{\underline{B}}_B(t + \Delta t) - A(\hat{\underline{q}}) \underline{B}_I(t + \Delta t) \right\}^T R^{-1} \left\{ \tilde{\underline{B}}_B(t + \Delta t) - A(\hat{\underline{q}}) \underline{B}_I(t + \Delta t) \right\} + \frac{1}{2} \underline{d}^T(t) W \underline{d}(t) \quad (30)$$

subject to

$$\hat{\underline{q}} = \frac{1}{2} \Omega(\hat{\underline{\omega}}) \hat{\underline{q}} = \frac{1}{2} \Xi(\hat{\underline{q}}) \hat{\underline{\omega}}, \quad \hat{\underline{q}}(t_0) = \underline{q}_0 \quad (31a)$$

$$\hat{\underline{H}} = \underline{N} - \left[J^{-1}(\hat{\underline{H}} - \underline{h}) \right] \times \hat{\underline{H}} + \underline{d}, \quad \hat{\underline{H}}(t_0) = \underline{H}_0 \quad (31b)$$

$$\hat{\underline{\omega}} = J^{-1}(\hat{\underline{H}} - \underline{h}) \quad (31c)$$

Since the body measurements ($\tilde{\underline{B}}_B$) are used as the required tracking trajectories, the output vector in Equation (18b) is given by

$$\underline{c}(\hat{\underline{x}}) = A(\hat{\underline{q}}) \underline{B}_I \quad (32)$$

where

$$\hat{\underline{x}} \equiv \begin{bmatrix} \hat{\underline{q}} \\ \dots \\ \hat{\underline{H}} \end{bmatrix} \quad (33)$$

Since \underline{c} depends on $\hat{\underline{q}}$ and not explicitly on $\hat{\underline{H}}$, the lowest order derivative of Equation (32) in which any component of \underline{d} first appears in $\hat{\underline{q}}$ is two, so that $p_i = 2$. Therefore, the $\underline{\Lambda}$, \underline{z} , \underline{b} , and \underline{e} quantities in Equation (22) are given by

$$\Lambda = \frac{\Delta t^2}{2} I \quad (34a)$$

$$\underline{z} = \Delta t \underline{L}_f^1 + \frac{\Delta t^2}{2} \underline{L}_f^2 \quad (34b)$$

$$\underline{b} = \Delta t \tilde{\underline{B}}_B + \frac{\Delta t^2}{2} \tilde{\tilde{\underline{B}}}_B \quad (34c)$$

$$\underline{e} = \tilde{\underline{B}}_B - A(\hat{q}) \underline{B}_I \quad (34d)$$

where

$$\left[\underline{L}_f^k \right]_i \equiv L_f^k(c_i) \quad (35)$$

Using the definitions in Equations (7), (14), and (16), the derivative of Equation (32) with respect to \hat{q} can be shown to be

$$\frac{\partial \underline{c}}{\partial \hat{q}} = -2 \Xi^T(\hat{q}) \Gamma(\underline{B}_I) \quad (36)$$

Therefore, \underline{L}_f^1 is given by

$$\underline{L}_f^1 = -\Xi^T(\hat{q}) \Gamma(\underline{B}_I) \Xi(\hat{q}) J^{-1} (\hat{H} - \underline{h}) \quad (37)$$

The derivative of Equation (37) with respect to \hat{q} is given by

$$\frac{\partial \underline{L}_f^1}{\partial \hat{q}} = 2[\hat{\omega} \times] \Xi^T(\hat{q}) \Gamma(\underline{B}_I) \quad (38)$$

The derivative of Equation (37) with respect to \hat{H} is given by

$$\frac{\partial \underline{L}_f^1}{\partial \hat{H}} = -\Xi^T(\hat{q}) \Gamma(\underline{B}_I) \Xi(\hat{q}) J^{-1} \quad (39)$$

Therefore, \underline{L}_f^2 is given by

$$\underline{L}_f^2 = [\underline{\hat{\omega}} \times] \Xi^T(\underline{\hat{q}}) \Gamma(\underline{B}_I) \Xi(\underline{\hat{q}}) \underline{\hat{\omega}} - \Xi^T(\underline{\hat{q}}) \Gamma(\underline{B}_I) \Xi(\underline{\hat{q}}) J^{-1} (\underline{N} - [\underline{\hat{\omega}} \times] \underline{\hat{H}}) \quad (40)$$

Comparing Equation (18a) and (31), the G matrix is given by

$$G = \begin{bmatrix} 0_{4 \times 3} \\ I_{3 \times 3} \end{bmatrix} \quad (41)$$

where $0_{4 \times 3}$ is a 4×3 zero matrix and $I_{3 \times 3}$ is a 3×3 identity matrix. The S matrix, which is formed using Equation (27) is given by

$$S = -\Xi^T(\underline{\hat{q}}) \Gamma(\underline{B}_I) \Xi(\underline{\hat{q}}) J^{-1} = [A(\underline{\hat{q}}) \underline{B}_I \times] J^{-1} \quad (42)$$

The 3×3 matrix $[A(\underline{\hat{q}}) \underline{B}_I \times]$ is analogous to the sensitivity matrix used in a Kalman filter (see [5]). This matrix has at most rank 2, which reflects the fact that there is no information about rotations around the current measurement vector. The extension to multiple measurement sets is achieved by stacking these measurements, e.g.,

$$\underline{e} = \begin{bmatrix} \underline{e}_1 \\ \underline{e}_2 \\ \vdots \\ \underline{e}_{m_{\text{sen}}} \end{bmatrix} \quad (43)$$

where m_{sen} is the total number of vector measurement sets available at time t_k .

An advantage of the nonlinear predictive filter over the conventional Kalman filter for attitude estimation shown in [5] is that quaternion normalization is always preserved. The normalization constraint leads to a singularity in the covariance matrix of the Kalman filter. Several methods are shown in references [5] and [9] which overcome this difficulty. However, since Equation (31a) is used to determine the quaternion estimate, and since the measurements only enter through the model error (\underline{d}) in Equation (31b), normalization is always maintained in the nonlinear predictive filter. Also, the predictive filter determines the model-error trajectory as part of the solution, as opposed to the Kalman filter which assumes that this error is modeled by a zero-mean Gaussian process with known covariance.

Inertial Reference Case

The quantity \underline{b} in Equation (34c) involves time derivatives of the body measurements. Since the body measurements invariably contain noise, the corresponding derivatives can be extremely corrupted by noise. In this section, the nonlinear predictive filter is re-derived by using the inertial reference vector as the “measurement.” The cost function for this case is given by

$$J = \frac{1}{2} \left\{ \underline{B}_I(t + \Delta t) - A^T(\hat{\underline{q}}) \tilde{\underline{B}}_B(t + \Delta t) \right\}^T R^{-1} \left\{ \underline{B}_I(t + \Delta t) - A^T(\hat{\underline{q}}) \tilde{\underline{B}}_B(t + \Delta t) \right\} + \frac{1}{2} \underline{d}^T(t) W \underline{d}(t) \quad (44)$$

subject to

$$\hat{\underline{q}} = \frac{1}{2} \Omega(\hat{\underline{\omega}}) \hat{\underline{q}} = \frac{1}{2} \Xi(\hat{\underline{q}}) \hat{\underline{\omega}}, \quad \hat{\underline{q}}(t_0) = \underline{q}_0 \quad (45a)$$

$$\hat{\underline{H}} = \underline{N} - \left[J^{-1}(\hat{\underline{H}} - \underline{h}) \right] \times \hat{\underline{H}} + \underline{d}, \quad \hat{\underline{H}}(t_0) = \underline{H}_0 \quad (45b)$$

$$\hat{\underline{\omega}} = J^{-1}(\hat{\underline{H}} - \underline{h}) \quad (45c)$$

The inertial reference vector is usually determined by an analytical model (e.g., the Earth’s magnetic field, the position of the sun or a star, etc.). Therefore, \underline{B}_I is not a stochastic process. However, this does not affect the filter’s performance. This can be shown by first assuming that the measurement errors in the body measurement vector ($\tilde{\underline{B}}_B$) are assumed isotropic, which leads to a measurement covariance matrix given by

$$R = r I_{3 \times 3} \quad (46)$$

where r is a scalar. From this assumption, it follows that the cost function in Equation (44) is identical to the cost function in Equation (30). Since the inverse of Equation (46) is used to weight the residual between the measurement and the estimate, \underline{B}_I is not required to be a stochastic process. The output vector in Equation (18b) is now given by

$$\underline{c}(\hat{\underline{x}}) = A^T(\hat{\underline{q}}) \tilde{\underline{B}}_B \quad (47)$$

The \underline{z} , \underline{b} , and \underline{e} quantities in Equation (22) are given by

$$\underline{z} = \Delta t \underline{L}_f^1 + \frac{\Delta t^2}{2} \underline{L}_f^2 \quad (48a)$$

$$\underline{b} = \Delta t \underline{\dot{B}}_I + \frac{\Delta t^2}{2} \underline{\ddot{B}}_I \quad (48b)$$

$$\underline{e} = \underline{B}_I - A^T(\underline{\hat{q}}) \underline{\tilde{B}}_B \quad (48c)$$

Using the definitions in Equations (7), (14), and (16), the derivative of Equation (47) with respect to $\underline{\hat{q}}$ can be shown to be

$$\frac{\partial \underline{c}}{\partial \underline{\hat{q}}} = -2 \Psi^T(\underline{\hat{q}}) \Omega(\underline{\tilde{B}}_B) \quad (49)$$

Therefore, \underline{L}_f^1 is given by

$$\underline{L}_f^1 = -\Psi^T(\underline{\hat{q}}) \Omega(\underline{\tilde{B}}_B) \Xi(\underline{\hat{q}}) J^{-1}(\underline{\hat{H}} - \underline{h}) \quad (50)$$

The derivative of Equation (50) with respect to $\underline{\hat{q}}$ is given by

$$\frac{\partial \underline{L}_f^1}{\partial \underline{\hat{q}}} = \Psi^T(\underline{\hat{q}}) \left[\Omega(\underline{\hat{\omega}}) \Omega(\underline{\tilde{B}}_B) - \Omega(\underline{\tilde{B}}_B) \Omega(\underline{\hat{\omega}}) \right] = 2 \Psi^T(\underline{\hat{q}}) \Omega(\underline{\tilde{B}}_B \times \underline{\hat{\omega}}) \quad (51)$$

where the identity in Equation (51) is formed from a Lie algebra group. The derivative of Equation (50) with respect to $\underline{\hat{H}}$ is given by

$$\frac{\partial \underline{L}_f^1}{\partial \underline{\hat{H}}} = -\Psi^T(\underline{\hat{q}}) \Omega(\underline{\tilde{B}}_B) \Xi(\underline{\hat{q}}) J^{-1} \quad (52)$$

Therefore, \underline{L}_f^2 is given by

$$\underline{L}_f^2 = \Psi^T(\underline{\hat{q}}) \Omega(\underline{\tilde{B}}_B \times \underline{\hat{\omega}}) \Omega(\underline{\hat{\omega}}) \underline{\hat{q}} - \Psi^T(\underline{\hat{q}}) \Omega(\underline{\tilde{B}}_B) \Xi(\underline{\hat{q}}) J^{-1} (\underline{N} - [\underline{\hat{\omega}} \times] \underline{\hat{H}}) \quad (53)$$

The S matrix, which is formed using Equation (27) is now given by

$$S = -\Psi^T(\underline{\hat{q}}) \Omega(\underline{\tilde{B}}_B) \Xi(\underline{\hat{q}}) J^{-1} = -A^T(\underline{\hat{q}}) [\underline{\tilde{B}}_B \times] J^{-1} \quad (54)$$

The 3×3 matrix $A^T(\hat{q})[\tilde{\underline{B}}_B \times]$ has at most rank 2, which again reflects the fact that there is no information about rotations around the current measurement vector. The advantage of the formulation shown in this section is that the time derivatives in Equation (48b) are not noisy.

Attitude Estimation-Angular Velocity Case

In this section, the nonlinear predictive filter is derived for spacecraft attitude using the quaternion kinematic equations and the angular velocity version of Euler's equation. The two cases of using body vector measurements and inertial reference measurements are shown. The angular velocity formulation shown in this section allows for direct estimation of the angular velocity, which may be desirable for control applications.

Body Measurement Case

The nonlinear predictive filter minimizes the following cost function

$$J = \frac{1}{2} \left\{ \tilde{\underline{B}}_B(t + \Delta t) - A(\hat{q})\underline{B}_I(t + \Delta t) \right\}^T R^{-1} \left\{ \tilde{\underline{B}}_B(t + \Delta t) - A(\hat{q})\underline{B}_I(t + \Delta t) \right\} + \frac{1}{2} \underline{d}^T(t) W \underline{d}(t) \quad (55)$$

subject to

$$\hat{\underline{q}} = \frac{1}{2} \Omega(\hat{\underline{\omega}}) \hat{\underline{q}} = \frac{1}{2} \Xi(\hat{\underline{q}}) \hat{\underline{\omega}}, \quad \hat{\underline{q}}(t_0) = \underline{q}_0 \quad (56a)$$

$$J \hat{\underline{\omega}} = \underline{N} - \underline{\dot{h}} - \hat{\underline{\omega}} \times (J \hat{\underline{\omega}} + \underline{h}) + \underline{d}, \quad \hat{\underline{\omega}}(t_0) = \underline{\omega}_0 \quad (56b)$$

The Λ , \underline{z} , \underline{b} , \underline{e} , and \underline{L}_f^1 quantities are again given by Equations (34) and (37). Also, the S matrix is again given by Equation (42). However, \underline{L}_f^2 is given by

$$\underline{L}_f^2 = [\hat{\underline{\omega}} \times] \Xi^T(\hat{\underline{q}}) \Gamma(\underline{B}_I) \Xi(\hat{\underline{q}}) \hat{\underline{\omega}} - \Xi^T(\hat{\underline{q}}) \Gamma(\underline{B}_I) \Xi(\hat{\underline{q}}) J^{-1} \{ \underline{N} - \underline{\dot{h}} - [\hat{\underline{\omega}} \times] (J \hat{\underline{\omega}} + \underline{h}) \} \quad (57)$$

Inertial Reference Case

The nonlinear predictive filter minimizes the following cost function

$$J = \frac{1}{2} \left\{ \underline{B}_I(t + \Delta t) - A^T(\hat{q}) \tilde{\underline{B}}_B(t + \Delta t) \right\}^T R^{-1} \left\{ \underline{B}_I(t + \Delta t) - A^T(\hat{q}) \tilde{\underline{B}}_B(t + \Delta t) \right\} + \frac{1}{2} \underline{d}^T(t) W \underline{d}(t) \quad (58)$$

subject to

$$\underline{\hat{q}} = \frac{1}{2}\Omega(\underline{\hat{\omega}})\underline{\hat{q}} = \frac{1}{2}\Xi(\underline{\hat{q}})\underline{\hat{\omega}}, \quad \underline{\hat{q}}(t_0) = \underline{q}_0 \quad (59a)$$

$$J\underline{\hat{\omega}} = \underline{N} - \underline{\hat{h}} - \underline{\hat{\omega}} \times (J\underline{\hat{\omega}} + \underline{h}) + \underline{d}, \quad \underline{\hat{\omega}}(t_0) = \underline{\omega}_0 \quad (59b)$$

The \underline{z} , \underline{b} , \underline{e} , and \underline{L}_f^1 vector quantities are again given by Equations (48) and (50). Also, the S matrix is again given by Equation (54). However, \underline{L}_f^2 is given by

$$\underline{L}_f^2 = \Psi^T(\underline{\hat{q}})\Omega(\underline{\tilde{B}}_B \times \underline{\hat{\omega}})\Omega(\underline{\hat{\omega}})\underline{\hat{q}} - \Psi^T(\underline{\hat{q}})\Omega(\underline{\tilde{B}}_B)\Xi(\underline{\hat{q}})J^{-1}\{\underline{N} - \underline{\hat{h}} - [\underline{\hat{\omega}} \times](J\underline{\hat{\omega}} + \underline{h})\} \quad (60)$$

Attitude Estimation of SAMPEX

In this section, the predictive filter used to estimate the attitude, rate, and input torque trajectories of the SAMPEX spacecraft using vector measurement observations. The SAMPEX general mission is to study energetic particles and various types of rays. The spacecraft is in a 550 by 675 km elliptical orbit with an 82° inclination. The attitude control hardware consists of a magnetic torquer assembly (MTA) and a single reaction wheel. The attitude determination hardware consists of five coarse sun sensors (CSS) (primarily for sun-acquisition), one fine sun sensor (FSS), and a three-axis magnetometer (TAM). Also, no rate sensing instruments are present on the spacecraft.

The onboard computer routine to determine attitude is based upon the TRIAD deterministic method. The spacecraft is controlled by the MTA to maintain the fixed solar arrays perpendicular to the sun-line. The reaction wheel is used to point the instrument boresight axis as required by the scientific mission. During eclipse no sun measurements are available from the FSS. Attitude control is maintained by using a constant sun-line vector as a “pseudo-measurement,” so that the reaction wheel is still utilized. During vector co-alignment, the spacecraft is placed in a “coast” mode in which neither the MTA nor the reaction wheel is used (see [13] for more details). The required nominal attitude determination accuracy is $\pm 2^\circ$. During anomalous conditions (eclipse and/or measurement vector co-alignment) the attitude cannot be determined by deterministic methods, such as TRIAD. The predictive filter presented in this

paper can determine the attitude in real-time using TAM measurements only, so that normal control procedures using the MTA and the reaction wheel can be maintained.

The inertial field trajectories are obtained by using a 8th order spherical harmonic model of the Earth’s magnetic field with International Geomagnetic Reference Field (IGRF) coefficients (see [14]). Magnetometer measurements by the TAM are known to be extremely accurate (within 0.3 mG). However, experience has shown that errors in the magnetic field model have a standard deviation of about 3 mG [7]. Therefore, 9 mG^2 is chosen for the diagonal elements of the measurement covariance matrix. For the FSS measurements, the primary source of error is the digitization noise of about 0.5° [7]. This error is assumed to be uniformly distributed so that the standard deviation of the FSS angle measurements is $0.5 \text{ deg}/\sqrt{12}$.

The formulation used to estimate for the attitude is given by Equations (58-60). This involves using the inertial reference sun and magnetic field trajectories as “measurements.” The angular velocity is estimated for by using Equation (59b). This equation involves a derivative term of the angular momentum due to the momentum wheel ($\dot{\underline{h}}$). The angular velocity measurement of the wheel contains a substantial amount of noise (see top of Figure 1). In order to filter this noise, the predictive filter is used as a linear filter with a simple second order plant which estimates for the angular velocity of the wheel and it’s derivative, given by

$$\begin{bmatrix} \hat{\underline{h}}(t) \\ \hat{\dot{\underline{h}}}(t) \end{bmatrix} = \begin{bmatrix} 0 & 1 \\ 0 & 0 \end{bmatrix} \begin{bmatrix} \underline{h}(t) \\ \hat{\underline{h}}(t) \end{bmatrix} + \begin{bmatrix} 0 \\ 1 \end{bmatrix} \underline{d}(t) \quad (61a)$$

$$\hat{\underline{h}}(t) = \begin{bmatrix} 1 & 0 \end{bmatrix} \begin{bmatrix} \hat{\underline{h}}(t) \\ \hat{\dot{\underline{h}}}(t) \end{bmatrix} \quad (61b)$$

The standard deviation of the wheel noise is about 1 rad/sec. A plot of the filtered wheel speed estimates is shown on the bottom plot of Figure 1. Clearly, the simple linear filter substantially reduces the noise in the wheel speed measurements.

Figure 1 Plot of the Measured and Filtered Wheel Speeds

The first test case involves using both TAM and FSS measurements. A plot of the finite differenced angular rates using TRIAD determined attitudes is shown in Figure 2. These rates

are extremely noisy, which is due to the large digitization noise associated with the FSS measurements. A plot of the predictive filter estimated rates using the same TAM and FSS vector measurements as in the TRIAD solution is shown in Figure 3. Clearly, these rates are smoother than the TRIAD determined rates. A plot of the determined input torques from the predictive filter is shown in Figure 4. These torques correspond to a correction to the dynamic model, so that the model responses match the vector measurement observations.

Figure 2 Plot of TRIAD Determined Angular Velocities

Figure 3 Plot of the Angular Velocity Estimates

Figure 4 Plot of the Determined Model Error Trajectories

The second case involves using TAM measurements only to estimate the attitude and angular rates. Since only one vector observation is used (i.e., TAM measurements only), a TRIAD solution is not possible. However, attitude estimation is possible using the predictive filter, since the filter utilizes Euler's equation for propagation. A plot of the estimated angular rate trajectories is shown in Figure 5. These angular rate estimates clearly show a rotation about the spacecraft's y-axis, which is the desired motion. A plot of the determined input torques from the predictive filter using TAM data only is shown in Figure 6. This again corresponds to a torque correction in Euler's equation. A plot of the error between the estimated attitudes using both TAM and FSS data in the predictive filter and the estimated attitudes using TAM only data in the predictive filter is shown in Figure 7. Although a true attitude is not known, this comparison can provide some insight into the accuracy of using a TAM only solution. From Figure 7, a slight hangoff is seen in the pitch axis. This may be due to nonlinear effects in the magnetic field model (see [15]). However, the predictive filter is able to determine attitudes to within 1° using TAM data only. This can be useful in determining the attitude when deterministic methods fail.

Figure 5 Plot of the Angular Velocity Estimates Using TAM Only

Figure 6 Plot of the Determined Model Error Trajectories Using TAM Only

Figure 7 Plot of Attitude Errors Between TAM/FSS and TAM Only

Conclusions

In this paper, a predictive filter was presented for use in real-time attitude estimation. This algorithm was specifically developed for spacecraft which lack angular rate sensing equipment. A number of formulations was presented which estimate for the spacecraft angular velocity or angular momentum. Also, algorithms are developed using either body measurements or inertial reference trajectories as the desired tracking trajectories. Using the inertial reference as the “measurement” avoids the need to take derivatives of noisy measurements. The advantages of the new algorithm over Kalman filter for attitude estimation include: (i) quaternion normalization is always preserved throughout the estimation process, (ii) actual model error trajectories are determined as part of the filter solution, and (iii) no covariance propagation is required, which leads to a computationally less demanding algorithm. The predictive filter was used to estimate the attitude of SAMPEX in order to demonstrate the usefulness of this algorithm. Results using SAMPEX data indicated that predictive filter provides a robust algorithm which can be used to determine the attitude of a spacecraft from magnetometer measurements only.

Acknowledgments

The first author’s work was supported by a National Research Council Postdoctoral Fellowship tenured at NASA-Goddard Space Flight Center. The author greatly appreciates this support. Also, the author wishes to thank Dr. D. Joseph Mook of the State University of New York at Buffalo for many interesting and helpful discussions.

References

- [1] Lerner, G.M., “Three-Axis Attitude Determination,” *Spacecraft Attitude Determination and Control*, edited by J.R. Wertz, D. Reidel Publishing Co., Dordrecht, The Netherlands, 1978, pp. 420-428.
- [2] Shuster, M.D., and Oh, S.D., “Attitude Determination from Vector Observations,” *Journal of Guidance and Control*, Vol. 4, No. 1, Jan.-Feb. 1981, pp. 70-77.

- [3] Markley, F.L., "Attitude Determination from Vector Observations: A Fast Optimal Matrix Algorithm," *The Journal of the Astronautical Sciences*, Vol. 41, No. 2, April-June 1993, pp. 261-280.
- [4] Wahba, G., "A Least-Squares Estimate of Satellite Attitude," Problem 65-1, *SIAM Review*, Vol. 7, No. 3, July 1965, pg. 409.
- [5] Lefferts, E.J., Markley, F.L., and Shuster, M.D., "Kalman Filtering for Spacecraft Attitude Estimation," *Journal of Guidance, Control and Dynamics*, Vol. 5, No. 5, Sept.-Oct. 1982, pp. 417-429.
- [6] Challa, M.S., Natanson, G.A., Baker, D.E., and Deutschmann, J.K., "Advantages of Estimating Rate Corrections During Dynamic Propagation of Spacecraft Rates-Applications to Real-Time Attitude Determination of SAMPEX," *Proceedings of the Flight Mechanics/Estimation Theory Symposium*, NASA-Goddard Space Flight Center, Greenbelt, MD, 1994, pp. 481-495.
- [7] Challa, M.S., *Solar, Anomalous, and Magnetospheric Particle Explorer (SAMPEX) Real-Time Sequential Filter (RTSF)*, Evaluation Report, NASA-Goddard Space Flight Center, Greenbelt, MD, April 1993.
- [8] Crassidis, J.L., and Markley, F.L., "A Minimum Model Error Approach for Attitude Estimation," submitted to the *Journal of Guidance, Control and Dynamics*.
- [9] Bar-Itzhack, I.Y., and Deutschmann, J.K., "Extended Kalman Filter for Attitude Estimation of the Earth Radiation Budget Satellite," *Proceedings of the AAS Astrodynamics Conference*, Portland, OR, August 1990, AAS Paper #90-2964, pp. 786-796.
- [10] Mook, D.J., and Junkins, J.L., "Minimum Model Error Estimation for Poorly Modeled Dynamic Systems," *Journal of Guidance, Control and Dynamics*, Vol. 3, No. 4, Jan.-Feb. 1988, pp. 367-375.
- [11] Lu, P., "Nonlinear Predictive Controllers for Continuous Systems," *Journal of Guidance, Control and Dynamics*, Vol. 17, No. 3, May-June 1994, pp. 553-560.
- [12] Kane, T.R., Likins, P.W., and Levinson, D.A., *Spacecraft Dynamics*, McGraw-Hill, New York, 1983.

[13] Flatley, T.W., Forden, J.K., Henretty, D.A., Lightsey, E.G., and Markley, F.L., "On-board Attitude Determination and Control for SAMPEX," *Proceedings of the Flight Mechanics/Estimation Theory Symposium*, NASA-Goddard Space Flight Center, Greenbelt, MD, 1990, pp. 379-398.

[14] Langel, R.A., "International Geomagnetic Reference Field: The Sixth Generation," *Journal of Geomagnetism and Geoelectricity*, Vol. 44, No. 9, 1992, pp. 679-707.

[15] Crassidis, J.L., Andrews, S.F., Markley, F.L., and Ha, K., "Contingency Designs for Attitude Determination of TRMM," *Proceedings of the Flight Mechanics/Estimation Theory Symposium*, NASA-Goddard Space Flight Center, Greenbelt, MD, 1995, pp. 419-433.

Figure 1 Plot of the Measured and Filtered Wheel Speeds

Figure 2 Plot of TRIAD Determined Angular Velocities

Figure 3 Plot of the Angular Velocity Estimates

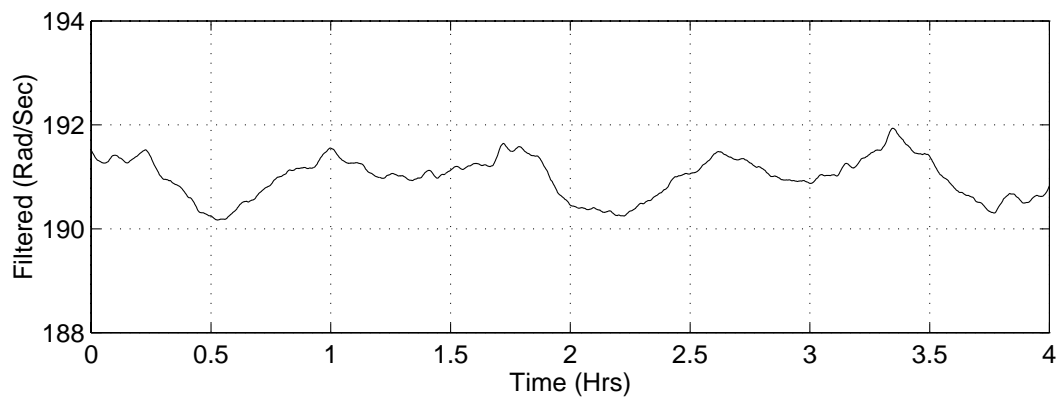
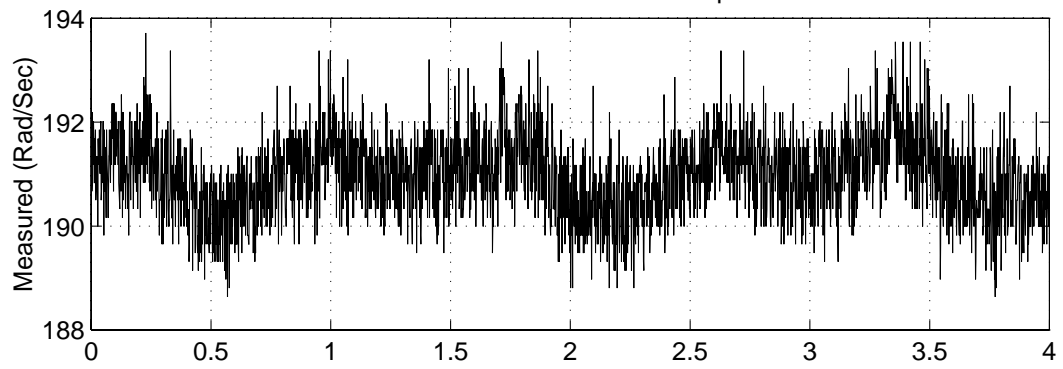
Figure 4 Plot of the Determined Model Error Trajectories

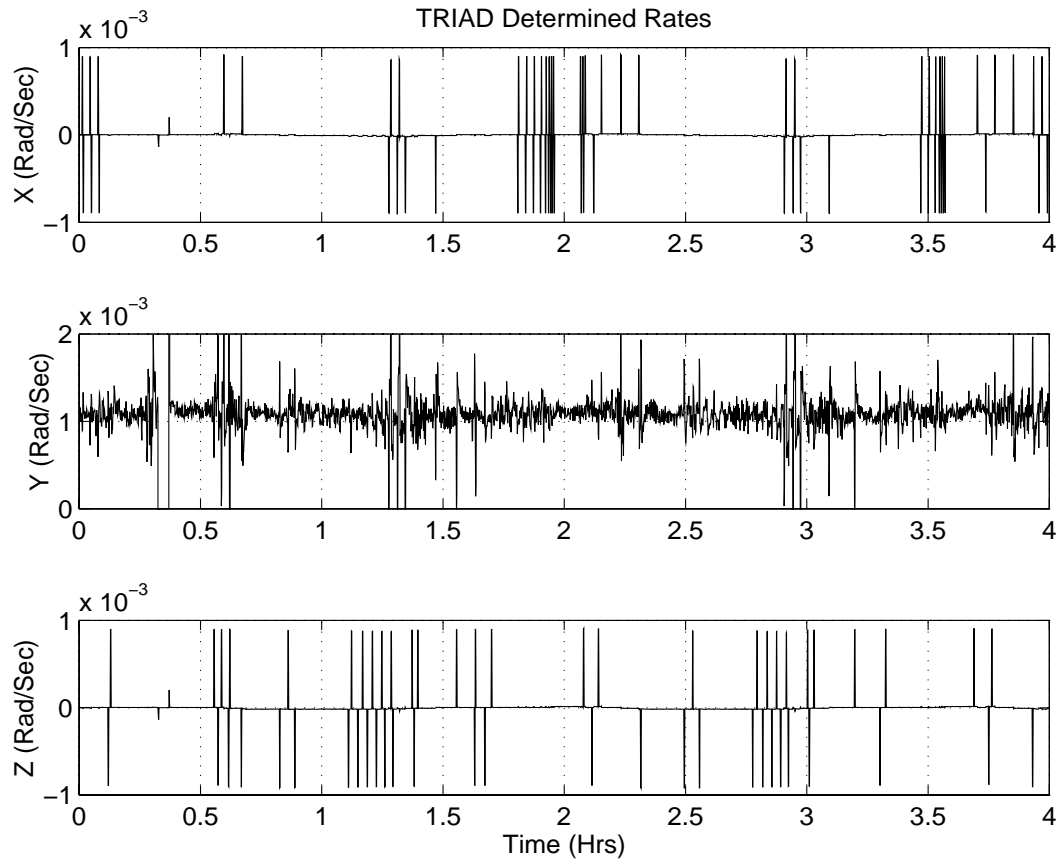
Figure 5 Plot of the Angular Velocity Estimates Using TAM Only

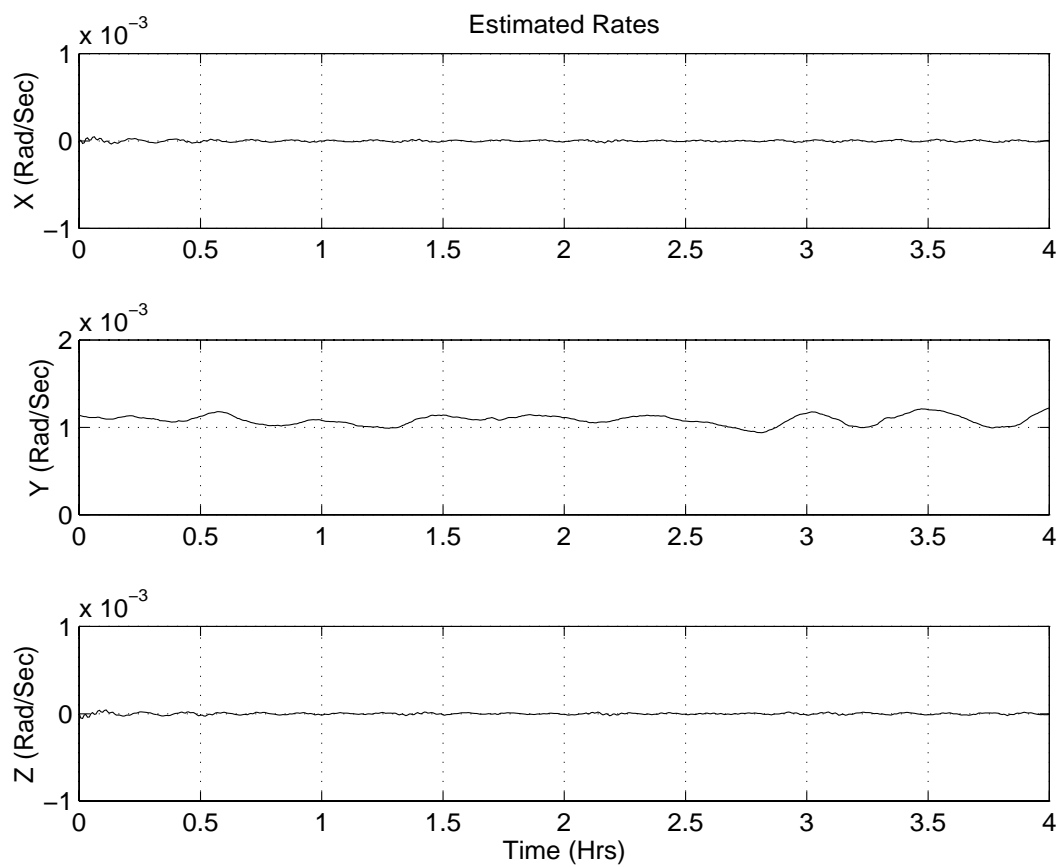
Figure 6 Plot of the Determined Model Error Trajectories Using TAM Only

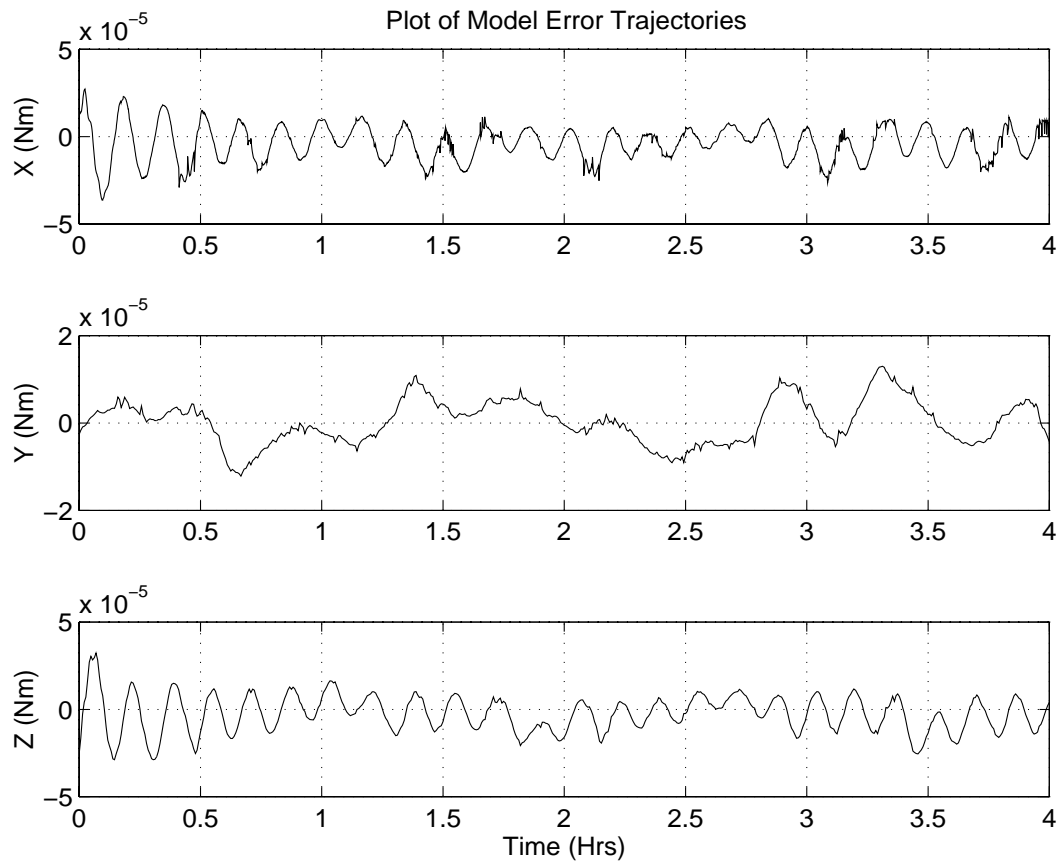
Figure 7 Plot of Attitude Errors Between TAM/FSS and TAM Only

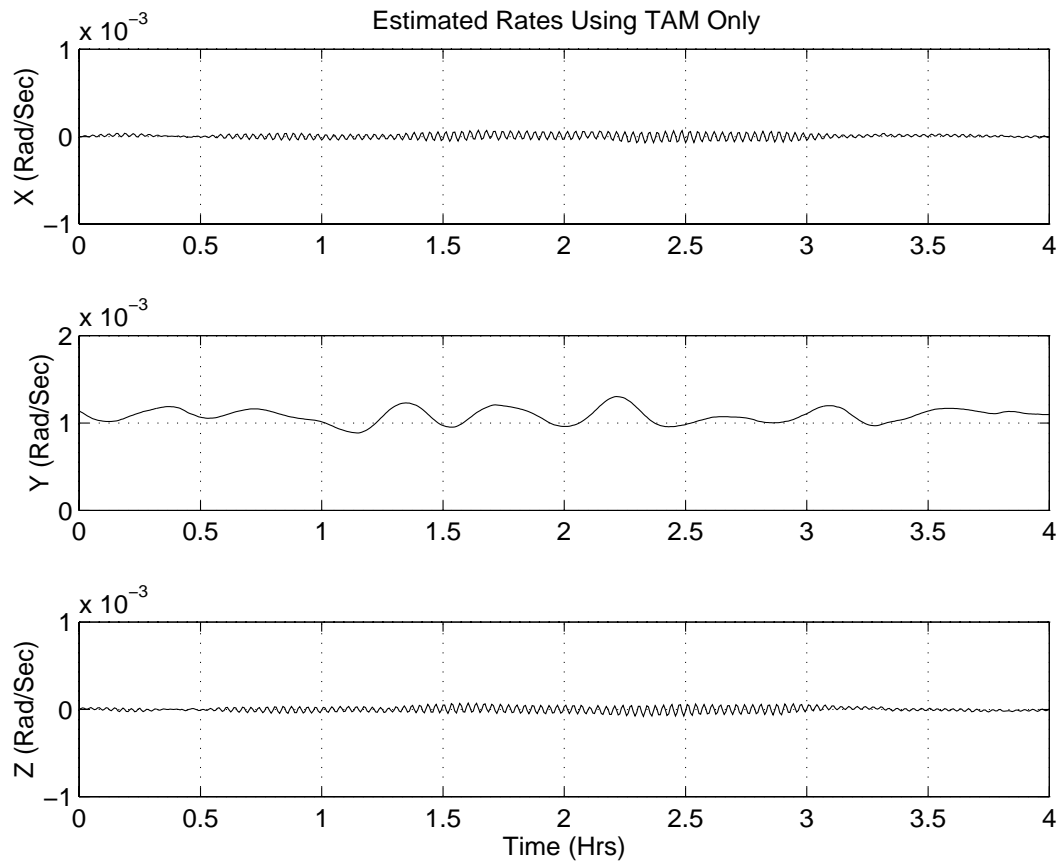
Measured and Filtered Wheel Speeds

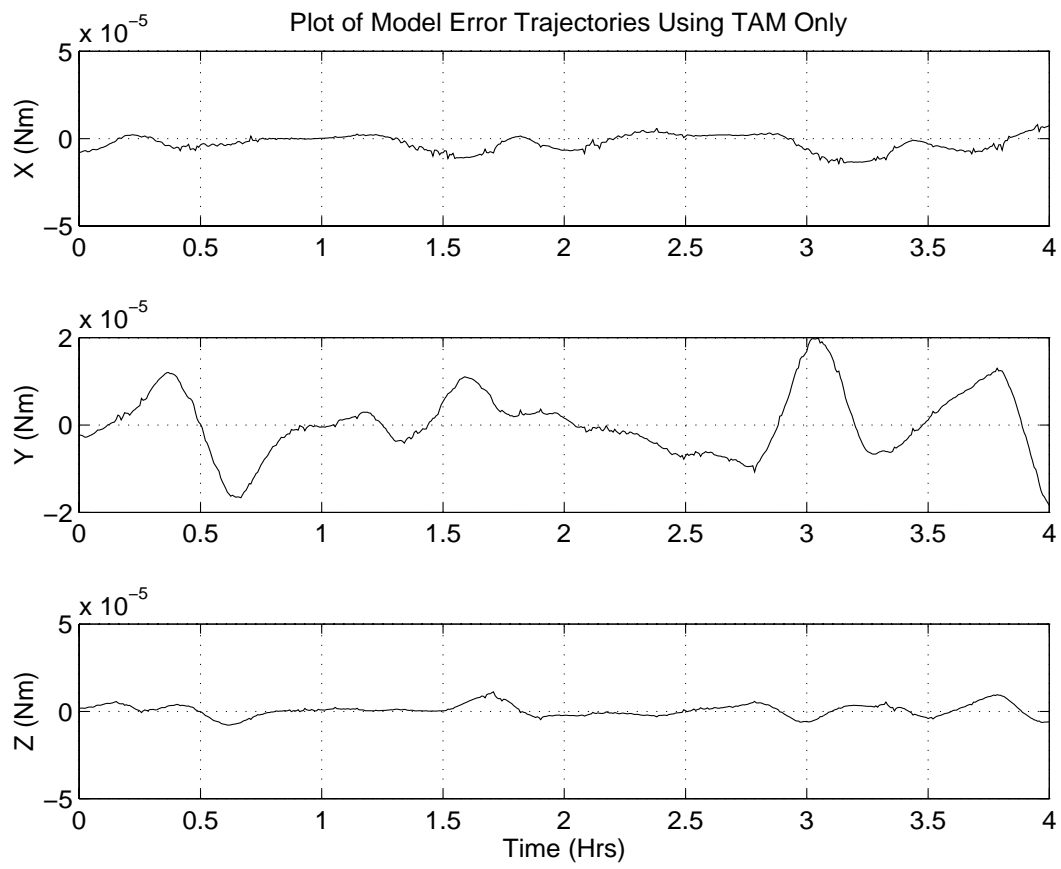












Error Angles Between TAM/FSS Attitudes and TAM Only Attitudes

